NASA CR-159,798

NASA CR-159798
IITRI-M6003-53

THERMAL FATIGUE AND OXIDATION DATA FOR DIRECTIONALLY SOLIDIFIED MAR-M 246 TURBINE BLADES

by

V. L. Hill and V. E. Humphreys
Materials Technology Division

IIT RESEARCH INSTITUTE
10 West 35 Street
Chicago, Illinois 60616

Prepared for

NATIONAL AERONAUTICS AND SPACE ADMINISTRATION

January 1980

CONTRACT NAS3-19696

NASA-Lewis Research Center
Cleveland, Ohio

Peter T. Bizon, Project Manager

1. Report No.	2. Government Accession No.	3. Recipient's Catalog No.
NASA CR-159798		

4. Title and Subtitle	5. Report Date
THERMAL FATIGUE AND OXIDATION DATA FOR DIRECTIONALLY SOLIDIFIED MAR-M 246 TURBINE BLADES	January 1980
	6. Performing Organization Code
7. Author(s)	8. Performing Organization Report No.
V. L. Hill and V. E. Humphreys	IITRI-M6003-53
	10. Work Unit No.
9. Performing Organization Name and Address	
IIT Research Institute 10 West 35 Street Chicago, Illinois 60616	11. Contract or Grant No. NAS3-19696
	13. Type of Report and Period Covered
12. Sponsoring Agency Name and Address	Contractor Report
National Aeronautics and Space Administration Washington, DC 20546	14. Sponsoring Agency Code

15. Supplementary Notes

Project Manager, Peter T. Bizon, Structures and Mechanical Technologies Division, NASA-Lewis Research Center, Cleveland, Ohio 44135

16. Abstract

Thermal fatigue and oxidation data were obtained for 11 plasma spray coated and 13 uncoated DS and single crystal MAR-M 246 blades. Blade coatings on the airfoil included several metal-oxide thermal barrier layers based on Al_2O_3, Cr_2O_3, or ZrO_2. The 24 turbine blades were tested simultaneously for 3000 cycles in fluidized beds maintained at 950° and 25°C using a symmetrical 360 sec thermal cycle.

In 3000 cycles, only uncoated turbine blades exhibited cracking on the trailing edge near the platform; 3 of the 13 uncoated blades did not crack. Cracking occurred over the range 400 to 2750 cycles, with single crystal blades indicating the poorest thermal fatigue resistance.

Oxidation of the uncoated blades was limited in 3000 cycles. All coatings indicated microscopically visible spalling at the trailing edge radius after 3000 cycles. Severe general spalling on the airfoil was observed for two multilayered coatings.

17. Key Words (Suggested by Author(s))		18. Distribution Statement
Thermal fatigue	Coatings	Unclassified - unlimited
Nickel alloys	Oxidation	
Turbine blades	Fluidized bed	
Heat resistant alloys	Directional Solidification	
Thermal resistance		

19. Security Classif. (of this report)	20. Security Classif. (of this page)	21. No. of Pages	22. Price*
Unclassified	Unclassified	39	

* For sale by the National Technical Information Service, Springfield, Virginia 22161

N80-21330#

FOREWORD

This report, NASA CR-159798, "Thermal Fatigue and Oxidation Data for Directionally Solidified MAR-M 246 Turbine Blades," summarizes the results of thermal fatigue testing of 24 coated and uncoated MAR-M 246 turbine blades. Work herein was conducted on Contract NAS3-19696 during the period 1 July 1978 to 1 October 1979. All testing on this program was conducted in the IITRI 50 kW fluidized bed with heating and cooling over the range 950°/25°C (1742°/77°F) for 3000 cycles. Other thermal fatigue data generated in this facility have been reported in NASA CR-72738, CR-121211, CR-121212, CR-134775, CR-135272, and CR-135299.

Work on this program was supported under Contract NAS3-19696 with P. T. Bizon of NASA-Lewis Research Center as the Project Monitor. IITRI personnel contributing to the program included V. L. Hill, Project Manager, and V. E. Humphreys, Project Engineer. Editorial and clerical support were provided by V. E.Johnson and M. Dineen, respectively. Data included in the report are contained in IITRI logbooks C23867 and C24095.

This report has been given the internal designation IITRI-M6003-53 (formerly B6135).

V. E. Humphreys
Assistant Metallurgist

V. L. Hill
Senior Scientific Advisor

M. A. H. Howes, Director
Materials Technology

TABLE OF CONTENTS

LIST OF TABLES

LIST OF FIGURES

SUMMARY

This report, NASA CR-159798, describes the results of thermal fatigue and oxidation testing of 24 coated and uncoated DS MAR-M 246 turbine blades. All testing was performed employing fluidized bed heating and cooling. Other thermal fatigue data generated in this facility have been reported in NASA CR-72738, CR-121211, CR-121212, CR-134775, CR-135272, and CR-135299.

Thermal fatigue and oxidation data were obtained for 11 plasma spray coated and 13 uncoated DS and single crystal MAR-M 246 blades. Blade coatings on the airfoil included several metal-oxide thermal barrier layers based on Al_2O_3, Cr_2O_3, and ZrO_2. The 24 turbine blades were tested simultaneously for 3000 cycles in fluidized beds maintained at 950° and 25°C using a symmetrical 360 sec thermal cycle. Cracking was determined by visual examination of test specimens. Thermocouple calibration of duplicate blades with 10 thermocouples each was conducted for three different thermal cycles.

In 3000 cycles, only uncoated turbine blades exhibited cracking; 3 of the 13 uncoated blades did not crack. Two of the three uncoated blades that did not crack were etched DS blades. All thermal fatigue cracks occurred on the trailing edge near the platform. Cracking of uncoated blades occurred over the range 400 to 2750 cycles, with single crystal blades indicating the poorest thermal fatigue resistance. Two of the three single crystal MAR-M 246 blades cracked in 400 cycles. Cracks in the platform were detected in seven coated and three uncoated blades after 3000 cycles.

Oxidation of the uncoated blades was limited in 3000 cycles at 950°/25°C; etched DS blades exhibited the best oxidation resistance. Coated blades exhibited weight loss due to spalling of the coatings. Severe general spalling on the airfoil was observed for two multilayered coatings based on Ni-20Cr/ZrO_2-5CaO after 3000 cycles. All coatings indicated microscopically visible spalling at the trailing edge radius after 3000 cycles.

1. INTRODUCTION

This report, NASA CR-159798, summarizes the thermal fatigue behavior of 24 MAR-M 246 turbine blades cycled 3000 times in fluidized beds maintained at 950° and 25°C. Thirteen of the blades were uncoated. The eleven coated blades consisted of plasma-sprayed thermal barrier coatings based on zirconia, chromia, or alumina as the barrier layer. All coatings were multilayer with a Ni-20Cr or NiCrAlY underlayer on the blade substrate.

Prior to thermal cycling, three calibration tests were conducted using ten chromel-alumel thermocouples mounted on calibration specimens. Calibration tests were conducted on two blades for each selected thermal cycle. Temperature transients were measured during cycling at seven locations on the blade section and three locations on the root area below the platform. Based on the calibration tests, thermal cycling was conducted using a 180 sec heating and 180 sec cooling cycle (360 sec total cycle) at 950°/25°C.

The turbine blade configuration evaluated in this program is that employed for the first stage space shuttle main engine high pressure fuel turbopump. Turbine blades were manufactured by Rocketdyne Division of Rockwell International. Coated blades were received with the coatings applied on the airfoil above the platform ready for thermal fatigue testing. The only modification of the blades conducted by IITRI was notching of the root section to anchor the blades in the thermal fatigue fixture.

Thermal fatigue data obtained previously in the IITRI fluidized bed facility on Contracts NAS3-17787 and NAS3-18942 have been reported in NASA CR-134775,[1] CR-135272,[2] and CR-135299.[3] Other data obtained on Contract NAS3-14311 are reported in NASA CR-72738,[4] CR-121211,[5] and CR-121212.[6] This effort comprises part of a general study of thermal fatigue being conducted by the NASA-Lewis Research Center. Further details of the study have been reported by Spera at al.,[7,8] Bizon et al.,[9-11] and Howes.[12]

Any material exposed to repeated temperature transients is subject to tensile failure by thermal fatigue, sometimes also defined as thermal shock. The thermal fatigue degradation mechanism involves accumulation of damage during multiple thermal cycles. Thermal shock, on the other hand, generally involves failure in relatively few cycles. The difference generally lies in the tensile ductility of the material within the temperature range of the imposed thermal cycle. Ductile materials tend to fail by thermal fatigue, whereas brittle materials fracture by thermal shock.

Material properties, other than ductility, important in thermal fatigue are hot tensile strength, elastic modulus, thermal conductivity, and thermal expansion. Oxidation

resistance apparently also plays a role in thermal fatigue. The interrelationship of material properties, the imposed thermal cycle, and component geometry defines the ability of a structure to resist thermal fatigue. However, the synergistic effects of these variables are quite complex and prediction of thermal fatigue behavior from basis properties is difficult. A major objective of the current NASA fatigue program is to develop and verify a viable statistical model for thermal fatigue by comparing experimental data with computer-derived predictions of thermal fatigue life.

A significant contribution to thermal fatigue results from geometry changes of a component. Generally, thermal fatigue failure results from the imposition of a tensile stress on a thin section by adjoining thick sections of a component or specimen. Aircraft turbine blades designed for minimum airfoil mechanical stresses have relatively little difference in cross-section in the gas path region, i.e., on the airfoil. For this reason, small aircraft turbine blades are resistant to thermal fatigue failures. When thermal fatigue cracking does occur, it tends to localize at the thinnest blade section with the greatest thermal gradient (i.e., at the trailing edge) near the blade root. Thermal cracking in the upper blade sections is difficult to obtain because of the inability to develop significant thermal gradients in the thin blade cross-section.

Thermal fatigue data in this report were generated using a multiple retort fluidized bed test facility consisting of one heating bed and two cooling beds. Glenny and co-workers reported the first use of fluidized beds to study thermal fatigue.[13] Fluidized bed heating and cooling provides very rapid heat transfer for both portions of the thermal cycle. An additional advantage of the fluidized bed method is that it provides a ready means of exposing a number of samples under identical test conditions. In this program, 24 turbine blades were exposed simultaneously.

The objective of the thermal fatigue test program was threefold:

1. Determine the number of imposed thermal cycles to initiation of blade cracking.

2. Obtain data on the rate of propagation of the cracks.

3. Generate qualitative weight change data for the various materials.

2. MATERIALS AND PROCEDURES

2.1 Experimental Procedure

Thermal cycling was conducted in the 50 kW IITRI fluidized bed thermal fatigue facility shown in Fig. 1. This facility, employing air as the fluidizing medium, was capable of cycling all 24 turbine blades simultaneously over the range 950°/25°C. Although the equipment contains two cooling beds, only one cooling bed was employed in this program. All 24 turbine blades were held in a single fixture.

The thermal fatigue fixture and fixture support are shown in Fig. 2. Turbine blades were held in a simulated turbine wheel in two tiers; the upper tier was offset from the lower tier to avoid restriction of fluidizing air to the upper tier. A conical air deflector was located at the bottom of the fixture to direct fluidizing air over the turbine blades. During thermal fatigue testing, blades were held with the leading edges downward as shown in Fig. 2b. This positioning was intended to provide a fluidizing air path similar to the gas path in the engine. At each inspection period blades were replaced in the fixture randomly to avoid any potential effects of position in the fixture on thermal fatigue behavior.

During thermal fatigue testing, samples were removed from testing at 25, 50, 100, 200, 300, 500, 700, 1000, 1500, 2000, 2500, and 3000 accumulated cycles for visual examination and gravimetric analysis. Visual examination was conducted using a 30X binocular microscope to determine the initiation of cracking and measurement of crack lengths. This technique permitted detection of cracks in excess of 0.25 mm (0.01 in.). Other detection techniques, such as dye penetrant inspection, could not be employed because of the roughened surface of the coatings and oxide layers on uncoated blades. Furthermore, it was intended to avoid contamination of the blade surfaces by inspection fluids. Visual measurement of thermal fatigue cracking has been extensively employed at IITRI in previous programs.

2.2 Specimen Identification

The manufacturer's identification (serial number) of the 24 turbine blades is summarized in Tables 1 and 2. Table 1 also contains data supplied by the manufacturer on coating composition and thickness for coated blades. No measurements of coating thickness were conducted at IITRI, nor was any metallographic examination made after thermal fatigue testing to verify coating thickness. It is understood that the coated blades were directionally solidified MAR-M 246 as the substrate alloy.

Uncoated blade identification data in Table 2 are also those of the blade fabricator. Blades 21-24 were in the etched condition to identify orientation of the directionally solidified grains. No effect of grain orientation on thermal fatigue was obtained in this program.

2.3 Thermocouple Calibration

Temperature transients were measured on two blades during thermal cycling at 950°/25°C prior to thermal fatigue testing. One calibration blade was inserted in both the upper and lower tier of the fixture; a full complement of 24 blades was included on this fixture during calibration tests. Three different calibration thermal cycles were used:

1. 120 sec heating-120 sec cooling (240 sec cycle)
2. 180 sec heating-120 sec cooling (300 sec cycle)
3. 180 sec heating-180 sec cooling (360 sec cycle).

In the course of the 240 sec and 300 sec cycle calibrations, the base of the blades below the platform was insulated with wrapped Fiberfrax. The insulation was intended to provide radial heat transfer in the blades during heating and cooling to maximize the gradients in the blade section above the platform.

Temperature calibration was conducted using ten thermocouples on each of the two blades. Thermocouples were 0.51 mm (0.020 in.) sheathed chromel-alumel thermocouples with 0.051 mm (0.002 in.) diameter thermocouple elements to maximize response. Locations of the ten thermocouples on the blades are shown in Fig. 3a; the final installation is shown in Fig. 3b. The locations were:

1. Trailing edge at blade tip
2. Trailing edge at mid chord
3. Trailing edge at platform
4. Leading edge at blade tip
5. Leading edge at mid chord
6. Leading edge at platform
7. Concave blade surface at centerline above platform
8. Trailing edge below platform

9. Leading edge below platform

10. Centerline of blade at root.

During calibration tests the fully loaded fixture completed three complete heating and cooling cycles prior to measurement of thermal transients. Temperatures were measured using Brush Model 816 multichannel recorders. During calibration and testing, blade samples were held with the leading edge at the bottom to simulate a fluidizing air path similar to the gas path in the turbopump.

All thermocouple junctions were spot welded to the turbine blades. Thermocouples located on the leading and trailing edges were spot welded as close to the edge as possible. However, because of the flatter contour near the trailing edge, it was possible to locate trailing edge thermocouples nearer the radius. After each calibration test all thermocouples were removed and replaced for the subsequent test. This was necessary to avoid thermocouple failures because the life of the 0.051 mm diameter thermocouple elements was limited at 950°C. Accordingly, the various thermocouples were located in the same area, but not necessarily in the exact same position for all calibration tests. This may have resulted in some deviation in behavior in comparison of temperature transients among the three calibration tests.

Temperatures during cycling were determined from the recorder strip charts at 3 sec intervals for the first 15 sec followed by 15 sec intervals to termination of heating or cooling. Data were then rounded to the nearest 5°C for each thermocouple in compiling the data in Tables 3 through 8.

3. EXPERIMENTAL RESULTS

3.1 Thermocouple Calibration

The results of calibration tests are summarized in Tables 3 through 8. Tables 3 and 4 contain transient data for the 360 sec symmetrical thermal cycle at 950°/25°C without root insulation. Results for 240 and 300 sec heating and cooling cycles are summarized in Tables 5 and 6, and 7 and 8, respectively. Insulation of the root area below the platform was used for both the 240 and 300 sec calibration tests.

Calibration data indicated more rapid heating of the trailing edge as expected. Insulation of the root area reduced heating and cooling rate at locations 8, 9, and 10, but did not significantly modify blade transients. Accordingly, the 360 sec total cycle without root insulation was selected and approved by the NASA project monitor for thermal fatigue testing.

3.2 Weight Change

At each inspection interval, all blades were weighed to indicate weight change due to oxidation and/or spalling. In the case of coated blades, weight change data were a measurement of spalling of the thermal barrier coatings due to thermal cycling. Weight change data, reported as percentage of the original weight of the blade, are summarized in Table 9. Figures 4 through 6 represent plots of the tabulated data in Table 9.

Generally, uncoated blades showed small weight losses, less than 0.1%, after 3000 cycles, except for blade No. 22 which exhibited a weight gain during the total 3000 cycle exposure. A weight loss of 0.1% represented about a 40 mg loss for the blade weights in this program. High weight losses were generally measured for coated blades due to spalling of the thermal barrier coating. In particular, blades 4 (multilayer Ni-20Cr + ZrO_2-5CaO), 6 (multilayer Ni-20Cr + 30(Ni-20Cr)-70(ZrO_2-5CaO) + ZrO_2-5CaO), and 7 (NiCrAlY + ZrO_2-12Y_2O_3) exhibited weight loss of 0.7 to 1.4%. Most of the remaining coated blades had weight losses of 0.07-0.5% except for blade 1 (Ni-20Cr + 50(Ni-20Cr)-50(ZrO_2-5CaO)) which had a weight gain of 0.06% at 3000 cycles. Loss of coating was readily visible for several blades, as will be shown subsequently.

Weight change data plotted versus accumulated cycles in Figs. 4 and 5 for coated blades is that of the individual blades. Data for uncoated blades presented in Fig. 6 are the averages of the three blades of each general category. Lowest weight loss occurred for the etched DS blades 21 to 24, with the other three groups of uncoated MAR-M 246 indicating similar weight change behavior. No difference in oxidation of directionally solidified and single crystal material was apparent.

3.3 Thermal Fatigue

Thermal fatigue cracking behavior of the 24 turbine blades at 950°/25°C is summarized in Table 10. Included in Table 10 are cycles to crack initiation and crack length, as well as the measured distance of the visibly observed crack from the tip of the turbine blade. Cracking in 3000 accumulated thermal cycles was limited to uncoated blades; all but three of the uncoated turbine blades cracked within 3000 cycles. None of the coated blades had visible cracks in 3000 cycles. It is possible that cracking of the coated blades occurred beneath the coating. This, however, could only be detected by post-exposure metallographic examination which was not within the scope of this program.

Data in Table 10 indicate that in most cases the blade cracks occurred on the trailing edge at, or near, the root of the airfoil at the platform. An exception was one of the two

cracks observed on blade 12 at 3000 cycles. The remaining blade cracks were observed at a distance of 17 to 24 mm from the blade tip; the blade length was approximately 25 mm at the trailing edge. Crack lengths were relatively short, less than 1.0 mm, and often cracks did not propagate significantly with accumulated thermal cycles. The estimated visible detection limit for cracks was 0.25 mm. Uncoated blades 14 (DS, unetched) and 21 and 22, both etched DS blades, did not crack in 3000 cycles at 950°/25°C.

In addition to blade cracks, 10 of the 24 blades exhibited cracks in the platform on the concave side of the blade at 3000 cycles, as shown in Table 10. The platforms were not coated, since thermal barrier coatings were limited to the airfoil. Of the 10 blades that exhibited platform cracks, 7 were coated blades; only coated blades 8, 9, 10, and 11 did not exhibit platform cracks at 3000 cycles. Uncoated blades that exhibited platform cracks were specimens 12, 19, and 21.

All platform cracks, which were previously noted to be located on the concave side of the blade, were generally located between the blade centerline and the leading edge. These cracks had generally propagated through the platform cross section to the blade surface. In some cases (blades 3, 12, 19, and 21) two cracks were observed in the platform.

Figures 7 to 10 show the surface appearance of the test blades as received. The appearance of the blades after 3000 cycles are shown in Figs. 11 to 14. Spalling of the coatings on the airfoils of blades 4 and 6 is readily apparent in Fig. 11. Localized spalling at the tip of the trailing edge on blade 7 can be seen in Fig. 12. For the remaining coated blades, localized spalling at the trailing edge radius was observed under the 30X microscope, although this effect is not evident in Figs. 11 and 12.

Figures 15 and 16 show typical thermal fatigue cracks at the trailing edge (blades 15 and 17) and on the platform (blades 12 and 21), respectively. Cracks in Fig. 15 were located on the radius of the trailing edge at the platform.

4. SUMMARY OF RESULTS

4.1 Oxidation Data

In general, oxidation of the uncoated directionally solidified MAR-M 246 after 3000 cycles at 950°/25°C was limited. No oxidation difference was apparent for DS or single crystal blades. Etched DS blades indicated measurably lower oxidation in 3000 cycles than unetched DS or single crystal blades. It is not known whether this observed effect would continue on further thermal cycling.

Weight loss of plasma-sprayed thermal barrier coated blades was due to spalling of the coatings. General spalling was apparent for blades 4 (multilayer Ni-20Cr + ZrO_2-5CaO) and 6 (multilayer Ni-20Cr + 30(Ni-20Cr)-70(ZrO_2-5CaO) + ZrO_2-5CaO) after 3000 cycles. All of the remaining blades indicated microscopically visible spalling, particularly at the radius of the trailing edge.

4.2 Thermal Fatigue

Table 11 summarizes the cycles to blade crack initiation for the 24 turbine blades through 3000 cycles at 950°/25°C using a 360 sec total thermal cycle. In this table, cycles to initiation of the first and second cracks was taken to be the mean of the last inspection without cracking and the first inspection that cracking was observed. Accordingly, if no cracking was observed at 2000 cycles, but was observed at 2500 cycles, the accumulated cycles to crack initiation was estimated to be 2250 cycles. As discussed previously, none of the coated blades exhibited blade cracking in 3000 cycles.

Data in Table 11 for the uncoated blades show variable thermal fatigue behavior for the various specimen groupings. For DS, blades 12-14, cycles to crack initiation varied from 800 to >3000 cycles. For the single crystal blades, 15-17, cycles to crack initiation ranged from 850 to 1250. These data were the most consistent of the four uncoated blade groups.

Blades 18-20 exhibited cracking over the range 400-2750 cycles, although blades 18 and 20 both cracked at 400 cycles. This group generally indicated the lowest thermal fatigue resistance of the uncoated blades; two of the three blades in this group cracked in 400 cycles. The difference between these blades and group 12-14 is not known.

Etched DS blades generally exhibited the best thermal fatigue resistance since two of the four blades of this type did not crack in 3000 cycles, and the third cracked at 2750 cycles. However, one of the etched DS blades, 23, did crack in 400 cycles; this difference is unexplainable without further metallurgical analysis. Etching of the DS blades 21-24 apparently improved both thermal fatigue and oxidation behavior.

Although thermal fatigue cracks did not propagate rapidly during thermal cycling in this program, axial loading due to turbine operation would likely modify crack propagation behavior. Imposition of more severe thermal transients than could be obtained in the fluidized bed would also probably reduce thermal fatigue life. Redesign of the blade to provide a more generous radius at the trailing edge may improve thermal fatigue life of the DS blades.

Platform cracking observed in this program is probably less significant than blade cracks observed. These cracks are not likely to be propagated by turbine operation; axial loading should not be significant. Since platform cracks were located near the leading edge, interaction with trailing edge cracks is not likely.

REFERENCES

1. Howes, M. A. H., "Thermal Fatigue Data on TAZ-8A, MAR-M 200, and Udimet 700 Superalloys," NASA CR-134775, 1975.

2. Hill, V. L., and Humphreys, V. E., "Thermal Fatigue and Oxidation Data of Superalloys Including Directionally Solidified Eutectics," NASA CR-135272, 1977.

3. Hill, V. L., and Humphreys, V. E., "Thermal Fatigue and Oxidation Data on Alloy/Braze Combinations," NASA CR-135299, 1977.

4. Howes, M. A. H., "Thermal Fatigue Data on 15 Nickel- and Cobalt-Base Alloys," NASA CR-72738, 1970.

5. Howes, M. A. H., "Additional Thermal Fatigue Data on Nickel- and Cobalt-Base Superalloys," Part 1, NASA CR-121211, 1973.

6. Howes, M. A. H., "Additional Thermal Fatigue Data on Nickel- and Cobalt-Base Superalloys," Part 2, NASA CR-121212, 1973.

7. Spera, D. A., and Grisaffe, S. J., "Life Prediction of Turbine Components: On-Going Studies at the NASA-Lewis Research Center," NASA TM X-2664, 1973.

8. Spera, D. A., Howes, M. A. H., and Bizon, P. T., "Thermal Fatigue Resistance of 15 High-Temperature Alloys Determined by the Fluidized-Bed Technique," NASA TM X-52975, March 1971.

9. Bizon, P. T., and Oldrieve, R. E., "Thermal Fatigue Resistance of NASA WAZ-20 Alloy with Three Commercial Coatings," NASA TM X-3168, 1975.

10. Bizon, P. T., and Spera, D. A., "Thermal-Stress Fatigue Behavior of Twenty-Six Superalloys," ASTM Special Technical Publication 612, 1976, pp. 106-122.

11. Bizon, P. T., and Spera, D. A., "Comparative Thermal Fatigue Resistance of Twenty-Six Nickel- and Cobalt-Base Alloys," NASA TN D-8071, 1975.

12. Howes, M. A. H., "Evaluation of Thermal Fatigue Resistance of Metals Using the Fluidized Bed Technique," ASTM Special Technical Publication 520, 1973, pp. 242-254.

13. Glenny, E., Northwood, J. E., Shaw, S. W. K., and Taylor, T. A., "A Technique for Thermal-Shock and Thermal-Fatigue Testing Based on the Use of Fluidized Solids," J. Inst. Metals, Vol. 87, 1958-1959, pp. 294-302.

Table 1

SPECIMEN IDENTIFICATION FOR PLASMA SPRAY COATED MAR-M 246 DS SPECIMENS

Blade No.	Serial No.	Casting Type	Composition, w/o	Thickness, mm
1	5T28	Base	Ni-20Cr	.025-.051
		Cover	50(Ni-20Cr)-50(ZrO_2-5CaO)[c]	.076-.101
2	5W21	Base	Ni-20Cr	.025-.051
		Cover	50(Ni-20Cr)-50Al_2O_3	.076-.101
3	5R6	Base	Ni-20Cr	.025-.051
		Cover	50(Ni-20Cr)-50Cr_2O_3	.076-.101
4	5M10	Multilayer[a]	Ni-20Cr	.025
			(ZrO_2-5CaO)[c]	.025
5	5R7	Multilayer[b]	NiCrAlY	.025
			(ZrO_2-12Y_2O_3)[d]	.025
6	4M28	Base	Ni-20Cr	.025-.051
		Cover 1	30(Ni-20Cr)-70(ZrO_2-5CaO)[c]	.089-.113
		Cover 2	(ZrO_2-5CaO)[c]	.063-.089
7	4D25	Base	NiCrAlY	.076-.101
		Cover	(ZrO_2-12Y_2O_3)[d]	.152-.203
8	5D17	Base	NiCrAlY	.025-.050
		Cover 1	30NiCrAlY-70(ZrO_2-12Y_2O_3)[d]	.089-.113
		Cover 2	(ZrO_2-12Y_2O_3)[d]	.063-.089
9	5N1	Base	NiCrAlY	.076-.101
		Cover	(ZrO_2-20Y_2O_3)[e]	.152-.203
10	5V15	Base	NiCrAlY	.076-.101
		Cover	(ZrO_2-20Y_2O_3)[e]	.152-.203
11	6X9	Base	NiCrAlY	.076-.101
		Cover	(ZrO_2-20Y_2O_3)[e]	.152-.203

[a]Six 0.025 mm thick layers (3 each) of Ni-20Cr and (ZrO_2-5CaO) beginning with Ni-20Cr.

[b]Six 0.025 mm thick layers (3 each) of NiCrAlY and (ZrO_2-12Y_2O_3) beginning with NiCrAlY.

[c]Norton 252.

[d]Zircoa.

[e]Metco.

Table 2

SPECIMEN IDENTIFICATION FOR UNCOATED TURBINE BLADES

Blade No.	Serial No.	Type
12	108	MAR-M 246 DS[a]
13	2N16	MAR-M 246 DS[a]
14	5K5	MAR-M 246 DS[a]
15	AA24	MAR-M 246 Single crystal[b]
16	AA25	MAR-M 246 Single crystal[b]
17	AA29	MAR-M 246 Single crystal[b]
18	Z20	MAR-M 246 DS[c]
19	Z28	MAR-M 246 DS[c]
20	Z32	MAR-M 246 DS[c]
21	4R24	MAR-M 246 DS[d]
22	4T12	MAR-M 246 DS[d]
23	5N24	MAR-M 246 DS[d]
24	2K1	MAR-M 246 DS[d]

[a]Not etched on airfoil.

[b]Identified RS00 7520-37.

[c]Identified RS00 7520-27.

[d]In etched condition.

Table 3

CALIBRATION DATA FOR TOP BLADE CYCLED AT 950°/25°C - 360 SEC CYCLE

Time, sec	Temperature at Thermocouple Position, °C																			
	Heating										Cooling									
	1	2	3	4	5	6	7	8	9	10	1	2	3	4	5	6	7	8	9	10
0	95	90	90	95	85	90	105	135	140	205	820	870	850	840	860	870	860	870	845	820
3	570	410	340	410	400	330	310	260	300	235	500	640	655	600	625	655	670	765	760	805
6	760	610	500	595	540	480	455	390	400	275	330	480	525	440	505	525	540	675	665	775
9	840	705	610	700	650	575	545	480	470	305	245	390	445	350	425	445	460	605	600	745
12	875	760	675	760	725	645	620	550	535	335	195	320	375	270	355	375	390	535	545	715
15	890	795	720	815	770	695	675	600	585	360	160	270	320	220	300	320	335	480	500	690
30	930	890	850	905	870	825	800	770	755	495	85	145	185	105	165	185	200	335	350	550
45	935	910	890	930	900	875	860	830	815	575	70	110	135	80	125	135	145	250	275	475
60	940	925	905	935	905	900	885	860	845	670	65	90	115	75	105	115	110	210	235	405
75	940	925	910	935	910	905	895	875	865	705	65	80	95	70	90	95	100	185	205	375
90	940	925	915	935	915	910	900	885	880	735	65	75	90	70	85	90	95	165	190	335
105	940	930	915	935	920	915	905	890	885	760	65	70	85	65	80	90	90	155	170	310
120	940	930	915	935	920	915	910	890	895	775	65	70	80	65	75	85	90	145	160	290
135	940	930	920	935	925	915	910	895	900	790	60	70	80	65	70	85	85	135	150	260
150	940	930	920	935	930	920	915	895	900	800	60	65	80	65	70	80	85	130	140	245
165	940	935	925	935	930	925	920	900	905	810	60	65	75	60	65	80	85	125	135	230
180	940	935	925	935	930	925	920	900	905	820	60	65	75	60	65	75	80	120	130	215

Table 4

CALIBRATION DATA FOR BOTTOM BLADE CYCLED AT 950°/25°C - 360 SEC CYCLE

Time, sec	Temperature at Thermocouple Position, °C																			
	Heating										Cooling									
	1	2	3	4	5	6	7	8	9	10	1	2	3	4	5	6	7	8	9	10
0	100	95	90	90	95	95	100	100	100	185	795	825	850	820	830	835	890	855	845	790
3	575	555	450	540	495	460	355	265	265	235	425	510	625	540	580	610	685	700	700	735
6	730	710	600	700	605	570	480	390	390	265	275	350	480	380	455	500	565	600	600	700
9	850	815	670	805	685	645	580	490	490	290	185	290	405	320	350	415	485	515	525	660
12	865	845	700	835	740	705	650	555	550	325	145	240	340	270	285	355	415	450	460	620
15	880	875	760	865	865	755	720	610	605	360	115	195	290	220	235	305	360	395	410	590
30	930	925	875	915	890	870	850	760	750	515	75	110	165	115	130	175	185	250	265	450
45	940	930	905	920	900	905	880	815	810	605	70	90	130	95	105	130	125	185	200	365
60	940	935	915	925	910	915	885	835	830	650	65	75	110	85	95	110	100	155	165	300
75	940	935	920	930	920	920	895	850	845	680	60	70	100	80	90	100	90	135	140	275
90	940	935	925	935	925	925	900	865	850	710	50	70	90	75	85	90	85	120	135	250
105	940	940	930	935	930	930	905	875	865	730	50	65	90	70	80	90	75	110	125	230
120	940	940	930	935	935	930	910	880	870	745	50	65	85	70	75	85	70	105	115	220
135	940	940	930	935	940	930	915	885	875	760	50	60	85	70	75	80	70	100	110	205
150	940	940	930	935	940	930	920	890	880	775	50	55	80	65	70	75	70	95	105	190
165	945	940	930	935	940	930	920	895	885	790	50	55	75	65	65	70	70	95	100	185
180	945	940	930	935	940	930	925	900	890	800	50	50	75	60	60	70	70	95	100	180

Table 5

CALIBRATION DATA FOR TOP BLADE CYCLED AT 950/25°C - 240 SEC CYCLE, INSULATED ROOT

Time, sec	Temperature at Thermocouple Position, °C																			
	Heating										Cooling									
	1	2	3	4	5	6	7	8	9	10	1	2	3	4	5	6	7	8	9	10
0	100	95	120	95	115	150	145	220	230	305	755	800	845	830	820	860	860	820	815	735
3	695	500	340	365	365	375	220	230	230	300	375	495	670	630	660	610	775	795	785	735
6	825	675	485	545	505	515	305	270	275	290	240	340	555	495	540	540	695	750	740	735
9	875	750	570	670	610	575	405	315	320	290	180	255	480	420	450	480	625	700	715	735
12	900	800	625	755	690	610	470	370	365	290	150	210	430	345	370	430	565	670	675	735
15	910	830	665	800	745	660	540	410	405	295	125	180	390	285	310	400	515	635	640	725
30	925	885	775	905	860	750	720	555	555	400	70	120	280	150	185	285	365	510	510	645
45	940	905	830	925	880	800	790	660	660	480	55	95	215	105	135	225	280	420	420	565
60	950	915	860	930	895	835	825	720	720	550	50	85	180	80	115	200	225	355	360	500
75	950	920	875	935	910	860	850	760	760	620	50	80	155	70	100	175	195	310	310	440
90	950	930	885	940	920	870	870	790	795	665	50	80	135	70	90	155	170	270	280	390
105	950	935	895	940	925	880	880	810	820	700	50	75	120	70	85	145	150	240	250	350
120	950	940	905	940	925	890	890	830	830	730	50	70	110	65	80	135	140	220	225	325

Table 6

CALIBRATION DATA FOR BOTTOM BLADE CYCLED AT 950/25°C - 240 SEC CYCLE, INSULATED ROOT

Time, sec	Temperature at Thermocouple Position, °C																			
	Heating										Cooling									
	1	2	3	4	5	6	7	8	9	10	1	2	3	4	5	6	7	8	9	10
0	110	100	135	90	110	145	155	205	245	285	790	820	855	825	810	865	865	795	800	675
3	685	510	425	420	385	380	240	220	245	285	390	505	610	620	675	620	770	750	790	675
6	765	680	540	560	525	520	325	265	265	285	250	350	505	485	530	545	690	710	760	675
9	815	755	610	680	615	585	415	315	310	285	185	270	435	390	435	490	630	670	730	675
12	845	800	660	760	700	630	480	360	340	290	155	220	380	310	360	440	560	635	700	665
15	865	820	700	815	755	675	550	400	385	295	130	190	345	260	305	395	510	610	675	655
30	915	880	795	900	870	780	730	545	520	355	80	125	260	135	180	290	360	495	545	600
45	925	900	825	915	890	820	780	635	615	435	70	100	205	95	135	230	285	410	455	535
60	930	905	850	920	905	850	815	690	675	505	65	90	175	80	110	195	230	350	390	470
75	930	910	865	925	915	870	825	735	725	570	60	80	160	70	95	170	200	305	340	425
90	935	920	880	930	920	880	840	765	760	620	55	75	135	70	85	155	175	270	305	385
105	935	925	890	935	925	890	855	790	785	655	55	70	125	70	80	140	155	240	270	345
120	940	930	900	940	930	895	870	810	805	680	55	65	120	65	75	135	145	215	245	310

Table 7

CALIBRATION DATA FOR TOP BLADE CYCLED AT 950/25°C - 300 SEC CYCLE, INSULATED ROOT

Time, sec	Temperature at Thermocouple Position, °C																			
	Heating										Cooling									
	1	2	3	4	5	6	7	8	9	10	1	2	3	4	5	6	7	8	9	10
0	105	105	155	100	105	150	170	240	255	360	790	810	855	830	850	865	880	865	875	815
3	690	560	420	460	430	410	265	260	265	355	350	550	670	600	640	670	800	835	865	815
6	815	670	520	620	550	535	350	300	310	355	220	410	575	440	525	570	715	795	805	815
9	870	735	600	720	630	610	435	355	355	360	170	350	500	365	440	505	645	755	765	810
12	900	780	655	775	685	660	495	400	405	360	135	290	440	305	370	455	585	715	730	805
15	920	815	695	810	725	705	560	440	445	365	110	240	385	260	320	410	535	680	700	795
30	935	870	820	875	850	825	735	590	605	430	70	170	280	175	205	310	380	540	565	785
45	940	890	840	895	875	850	805	680	690	515	65	130	225	135	155	235	300	455	470	635
60	940	900	865	905	880	870	835	735	745	595	60	105	185	115	125	195	255	395	405	565
75	945	905	885	910	900	885	860	780	785	650	55	85	165	95	110	175	220	345	355	505
90	945	910	895	915	910	895	880	805	810	690	55	75	150	85	100	160	195	305	320	455
105	945	915	905	920	915	900	890	825	830	725	55	65	135	80	90	145	175	275	295	410
120	945	920	910	925	920	905	900	840	840	745	50	60	130	75	85	135	160	255	270	380
135	945	925	915	930	925	910	905	850	855	770										
150	945	930	915	935	930	915	910	860	860	785										
165	950	935	920	940	935	915	910	870	870	805										
180	950	940	925	940	940	920	915	875	875	810										

Table 8

CALIBRATION DATA FOR BOTTOM BLADE CYCLED AT 950/25°C - 300 SEC CYCLE, INSULATED ROOT

Time, sec	Temperature at Thermocouple Position, °C																			
	Heating										Cooling									
	1	2	3	4	5	6	7	8	9	10	1	2	3	4	5	6	7	8	9	10
0	90	105	165	100	110	155	180	240	255	350	790	840	830	825	830	840	870	870	865	820
3	645	475	440	470	430	420	275	255	265	345	360	510	655	540	600	600	785	845	850	815
6	825	655	540	650	540	525	360	300	290	340	230	355	545	340	515	530	705	800	825	810
9	870	740	610	750	630	615	445	350	325	340	175	280	480	260	460	490	640	755	790	805
12	900	785	655	795	700	670	515	395	360	340	145	240	430	225	385	450	585	720	765	795
15	910	825	690	835	755	710	570	435	385	345	120	205	390	190	335	415	540	680	740	780
30	930	895	790	900	870	810	745	575	545	425	80	135	285	125	205	305	370	540	605	700
45	935	910	830	915	900	850	815	665	645	510	70	110	240	110	145	245	310	455	510	615
60	940	915	860	920	910	875	845	730	715	590	65	95	205	100	120	210	265	390	440	545
75	945	920	875	925	915	890	870	780	760	650	60	90	180	90	105	175	230	335	385	485
90	945	925	890	925	920	900	890	810	790	705	60	80	160	80	95	155	205	300	340	435
105	945	925	900	925	925	905	895	830	810	735	60	75	150	75	90	140	190	275	305	300
120	945	930	905	930	930	905	910	845	830	755	55	70	140	75	85	125	180	250	275	265
135	950	930	910	930	930	910	910	855	840	775										
150	950	930	915	935	935	915	915	865	850	790										
165	950	930	920	935	940	915	915	870	860	800										
180	950	935	925	940	940	920	920	875	865	810										

Table 9

WEIGHT CHANGE DATA FOR TURBINE BLADES

Blade Identification	Starting Weight, g	Weight Change at Given Cycle, %											
		25	50	100	200	300	500	700	1000	1500	2000	2500	3000
1	38.0107	.024	.035	.033	.038	.043	.041	.033	.033	.043	.053	.062	.057
2	37.5212	.011	.011	.014	.010	.010	-.001	-.025	-.042	-.060	-.111	-.27	-.41
3	37.9943	.011	.011	.006	-.005	-.011	-.030	-.058	-.085	-.109	-.131	-.158	-.198
4	38.2000	-.019	-.023	-.026	-.035	-.042	-.088	-.136	-.231	-.39	-.68	-1.03	-1.42
5	37.9150	-.037	-.048	-.066	-.091	-.115	-.148	-.199	-.243	-.28	-.33	-.39	-.47
6	38.2532	-.007	-.010	-.017	-.020	-.028	-.036	-.055	-.078	-.084	-.096	-.132	-.71
7	38.6649	-.192	-.203	-.215	-.230	-.248	-.269	-.31	-.35	-.38	-.42	-.47	-.82
8	39.2945	-.006	-.015	-.022	-.033	-.039	-.062	-.089	-.130	-.160	-.203	-.27	-.37
9	39.5246	-.050	-.062	-.082	-.096	-.107	-.136	-.170	-.229	-.26	-.30	-.34	-.42
10	38.8173	-.042	-.051	-.066	-.091	-.099	-.126	-.158	-.193	-.224	-.26	-.43	-.51
11	38.8291	-.029	-.040	-.055	-.076	-.095	-.126	-.157	-.197	-.231	-.28	-.35	-.43
12	34.9858	.001	.002	.004	.001	-.001	-.005	-.012	-.021	-.028	-.038	-.049	-.074
13	35.0430	.004	.003	.003	.002	-.003	-.007	-.024	-.033	-.039	-.043	-.064	-.080
14	35.1743	.004	.003	.003	.002	-.003	-.007	-.020	-.026	-.032	-.036	-.055	-.072
15	37.9475	.002	.003	.004	-.001	-.002	-.010	-.027	-.037	-.043	-.056	-.072	-.105
16	37.7740	.003	.003	.002	.001	-.004	-.010	-.023	-.034	-.038	-.047	-.057	-.082
17	37.5285	.008	.005	.007	.005	.003	-.004	-.016	-.027	-.034	-.052	-.075	-.088
18	37.4493	.007	.006	.007	.007	.006	-.001	-.012	-.024	-.031	-.046	-.070	-.090
19	37.3410	.003	.003	.004	.001	.001	-.009	-.022	-.039	-.049	-.065	-.078	-.100
20	37.5552	.006	.008	.007	.006	.003	-.008	-.018	-.039	-.049	-.065	-.076	-.102
21	36.8587	0	.010	.014	.012	.016	.024	.028	.018	.019	.018	-.002	-.006
22	36.5595	.004	.007	.010	.009	.010	.011	.011	.007	.019	.025	.023	.015
23	36.1966	.002	.005	.009	.009	.007	.018	.023	.014	.016	.010	.007	-.030
24	35.2648	.005	.010	.009	.013	.009	.017	.017	.009	.009	.010	-.003	-.014

Table 10

SUMMARY OF CRACK INITIATION AND PROPAGATION FOR TURBINE BLADES

Blade No.	Cycles	Crack Length, mm			Total Cracks Observed
		1st Crack	2nd Crack	3rd Crack	
		Blade Cracks[a]			
12	2500	No cracks			0
	3000	0.25 (5.1)[b]	0.25 (21.6)[b]		2
13	700	No cracks			0
	1000	0.51 (24.1)			1
	1500	0.51 (24.1)			1
	2000	0.51 (24.1)			1
	2500	0.51 (24.1)			1
	3000	0.51 (24.1)			1
15	1000	No cracks			0
	1500	0.51 (24.1)			1
	2000	0.51 (24.1)			1
	2500	0.76 (24.1)	0.25 (14.0)		2
	3000	0.76 (24.1)	0.25 (14.0)		2
16	700	No cracks			0
	1000	0.51 (24.1)			1
	1500	0.51 (24.1)			1
	2000	0.51 (24.1)			1
	2500	0.76 (24.1)			1
	3000	0.76 (24.1)			1
17	1000	No cracks			0
	1500	0.25 (24.1)			1
	2000	0.51 (24.1)			1
	2500	0.51 (24.1)			1
	3000	0.51 (24.1)			1
18	300	No cracks			0
	500	0.25 (23.9)			1
	700	0.51 (23.9)			1
	1000	0.51 (23.9)			1
	1500	0.51 (23.9)			1
	2000	0.76 (23.9)			1
	2500	1.0 (23.9)			1
	3000	1.0 (23.9)			1
19	2500	No cracks			0
	3000	0.51 (23.4)			1
20	300	No cracks			0
	500	0.25 (17.8)			1
	700	0.25 (17.8)			1
	1000	0.25 (17.8)	0.76 (24.1)		2

Table 10 (cont.)

Blade No.	Cycles	Crack Length, mm 1st Crack	2nd Crack	3rd Crack	Total Cracks Observed
	1500	0.25 (17.8)	0.76 (24.1)		2
	2000	0.25 (17.8)	0.76 (24.1)		2
	2500	0.25 (17.8)	0.76 (24.1)		2
	3000	0.25 (17.8)	0.76 (24.1)		2
23	300	No cracks			0
	500	0.25 (22.8)	0.25 (19.1)		2
	700	0.51 (22.8)	0.25 (19.1)		2
	1000	0.51 (22.8)	0.25 (19.1)		2
	1500	0.51 (22.8)	0.25 (19.1)		2
	2000	0.51 (22.8)	0.25 (19.1)		2
	2500	0.51 (22.8)	0.25 (19.1)		2
	3000	0.51 (22.8)	0.25 (19.1)		2
24	2500	No cracks			0
	3000	0.25 (21.6)			1
		Platform Cracks[c]			
1	2500	No cracks			0
	3000	0.51 (10.2)[d]			1
2	2500	No cracks			0
	3000	0.76 (11.9)			1
3	2500	No cracks			0
	3000	0.76 (7.6)	0.51 (10.4)		2
4	2500	No cracks			0
	3000	0.25 (8.9)			1
5	2500	No cracks			0
	3000	0.51 (8.9)			1
6	2500	No cracks			0
	3000	0.25 (9.4)			1
7	2500	No cracks			0
	3000	0.51 (7.6)			1
12	2500	No cracks			0
	3000	0.76 (3.8)	1.0 (6.4)		2
19	2500	No cracks			0
	3000	0.25 (6.4)	0.51 (7.6)		2
21	2500	No cracks			0
	3000	1.3 (3.8)	0.76 (4.6)		2

[a] All cracks were located on the trailing edge.
[b] For blade cracks, distance from tip of blade is in parentheses.
[c] All cracks were located on concave side of blade.
[d] For platform cracks, distance from leading edge of blade is in parentheses.

Table 11

ACCUMULATED CYCLES TO THERMAL FATIGUE CRACKING OF MAR-M 246 TURBINE BLADES

Blade No.	Accumulated Cycles to Crack Initiation		Total No. of Cracks
	1st Crack	2nd Crack	
	Coated Blades		
1	>3000	>3000	0
2	>3000	>3000	0
3	>3000	>3000	0
4	>3000	>3000	0
5	>3000	>3000	0
6	>3000	>3000	0
7	>3000	>3000	0
8	>3000	>3000	0
9	>3000	>3000	0
10	>3000	>3000	0
11	>3000	>3000	0
	Uncoated Blades		
12	2750	2750	2
13	850	>3000	1
14	>3000	>3000	0
15	1250	2250	2
16	850	>3000	1
17	1250	>3000	1
18	400	>3000	1
19	2750	>3000	1
20	400	850	2
21	>3000	>3000	0
22	>3000	>3000	0
23	400	400	2
24	2750	>3000	1

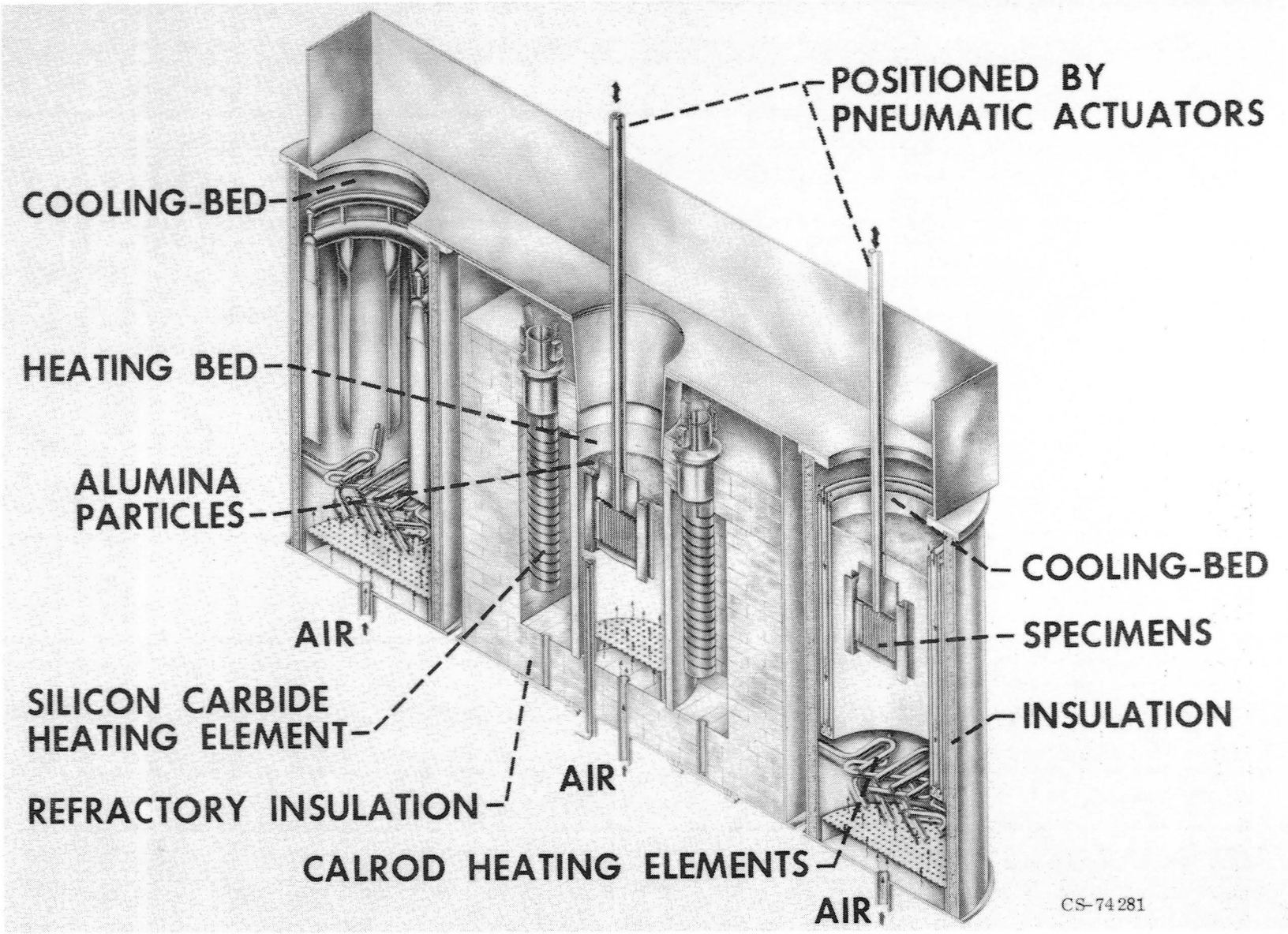

Figure 1
Fluidized Bed Thermal Fatigue Facility

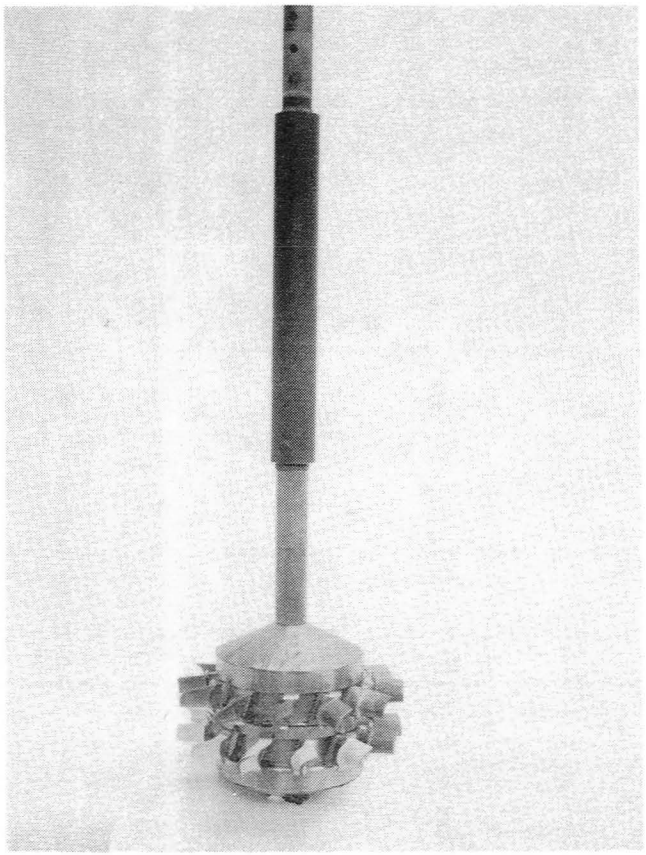

Neg. No. 48598 1/5X

(a) Fixture and support

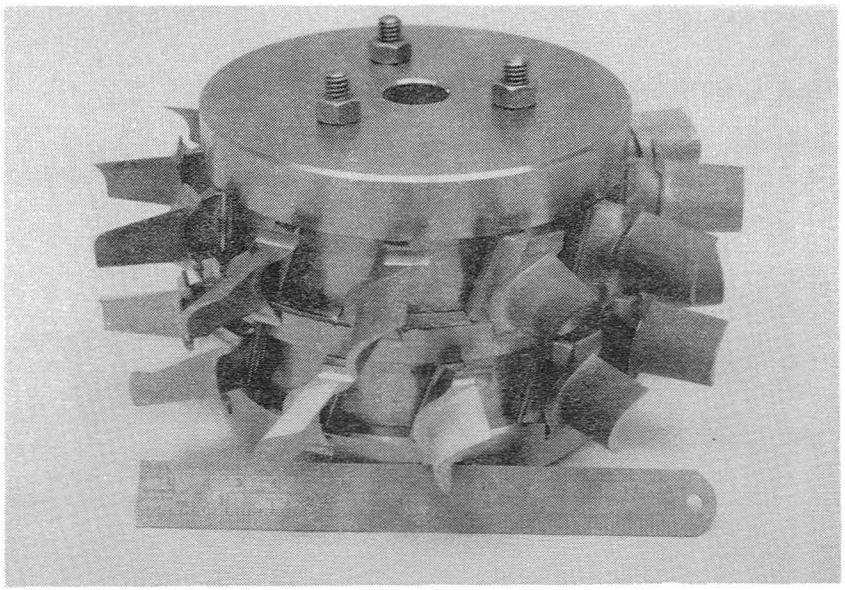

Neg. No. 48596 1/2X

(b) Test fixture

Figure 2

Experimental Design of Test Fixture

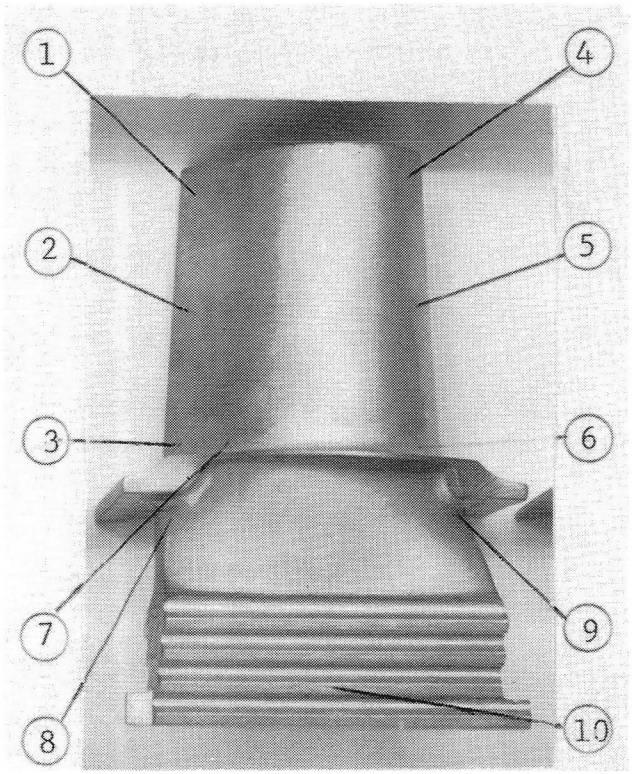

Neg. No. 48585 1.5X

(a) Thermocouple locations

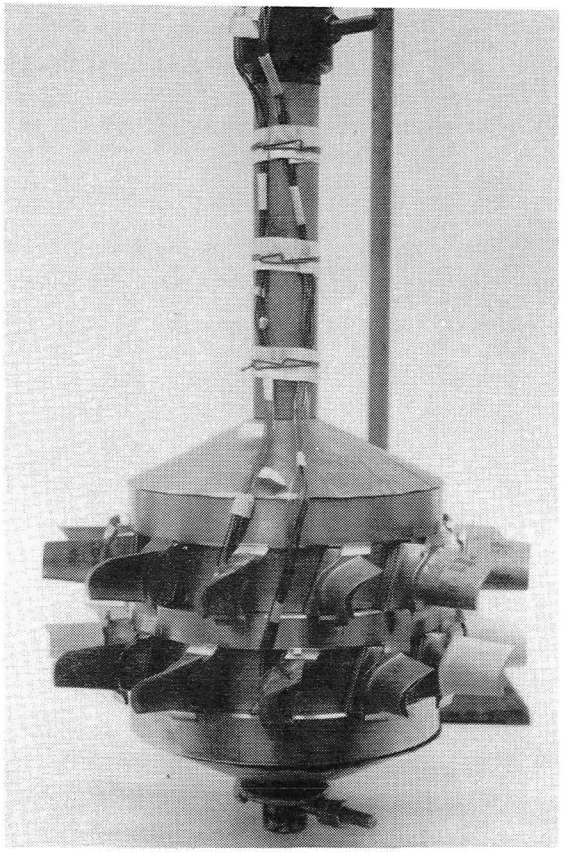

Neg. No. 48651 1/2X

(b) Thermocouple installation

Figure 3

Experimental Design for Calibration Tests
Showing Attachment of Ten Thermocouples

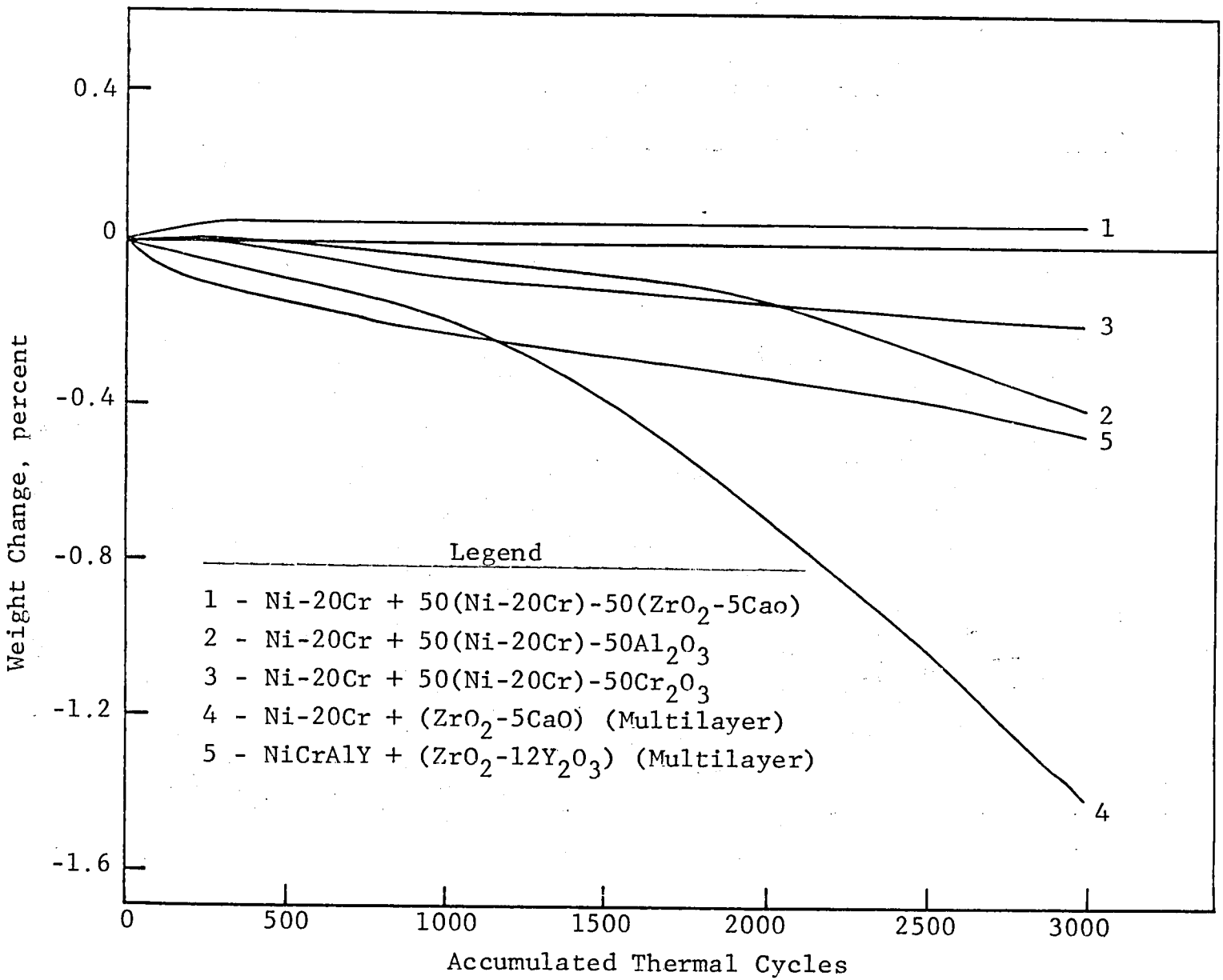

Figure 4

Percent Weight Change versus Accumulated Thermal Cycles for Plasma Spray Coated Blades 1-5

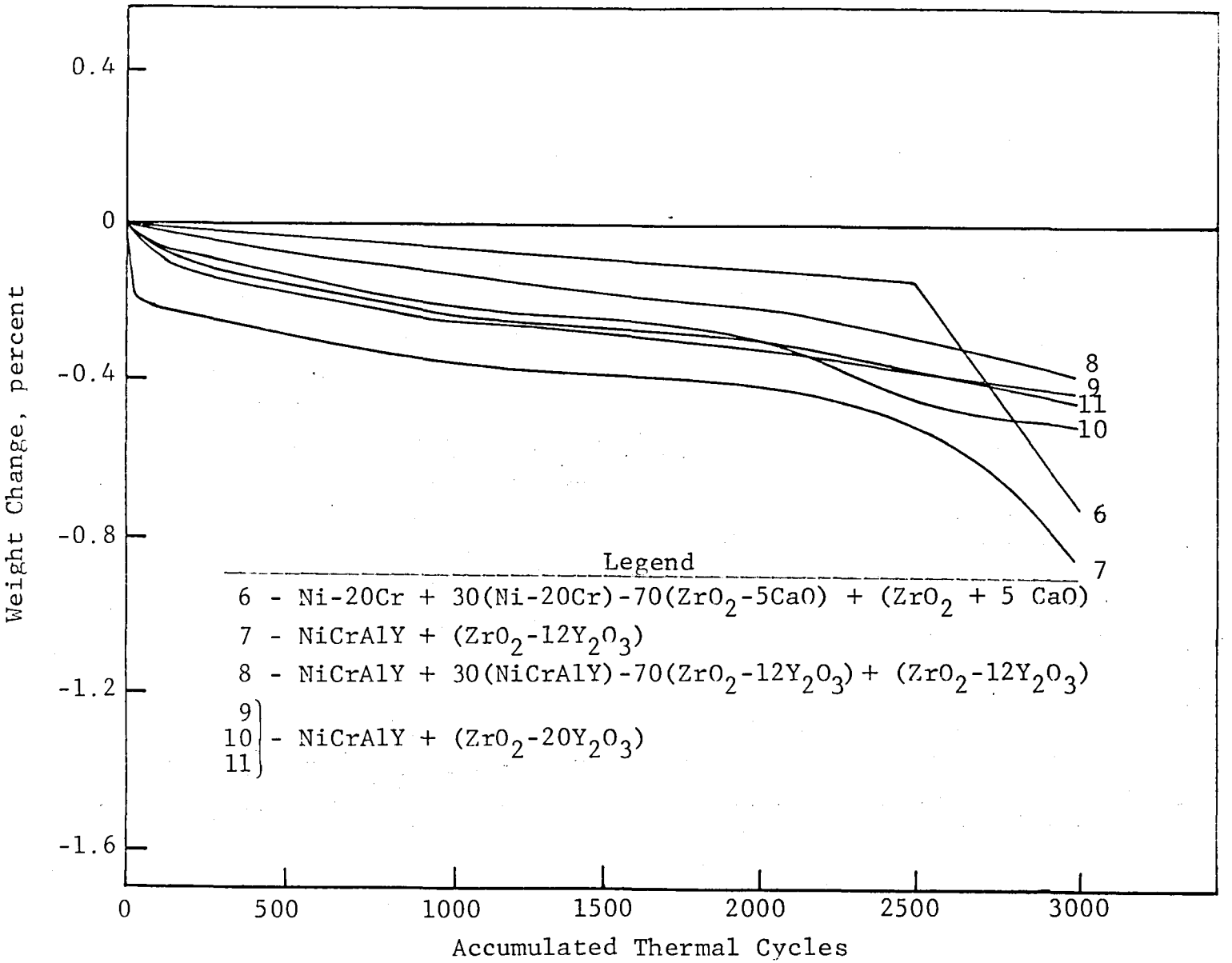

Figure 5

Percent Weight Change versus Accumulated Thermal Cycles for Plasma Spray Coated Blades 6-11

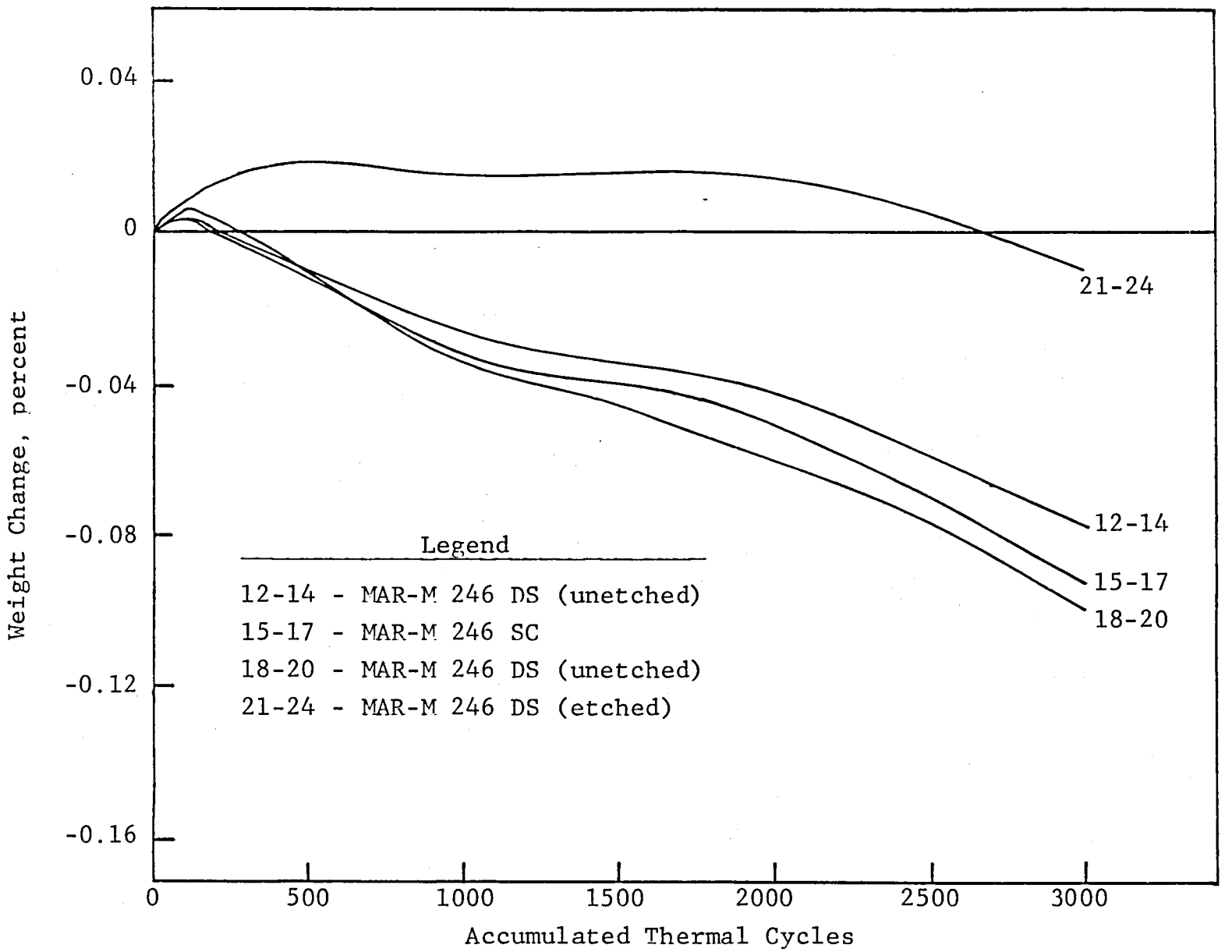

Figure 6

Percent Weight Change versus Accumulated Thermal Cycles
for Uncoated Turbine Blades 12-24

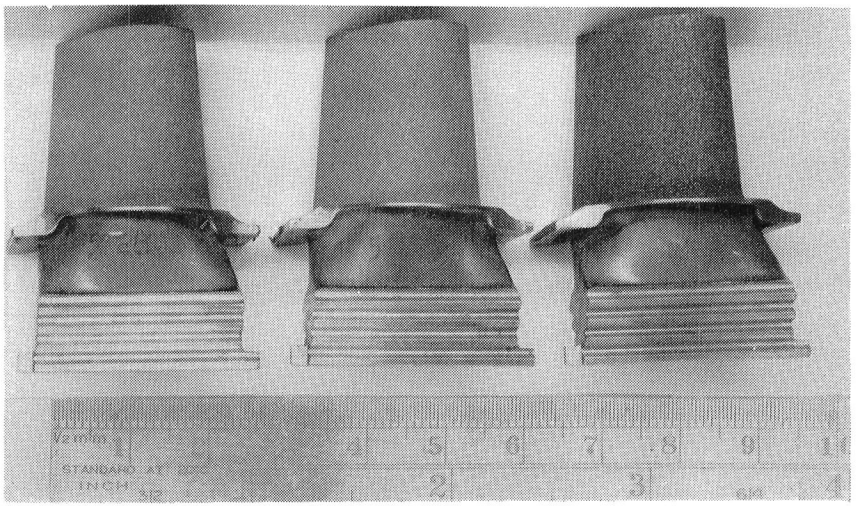

Neg. No. 48592 1X

1 2 3

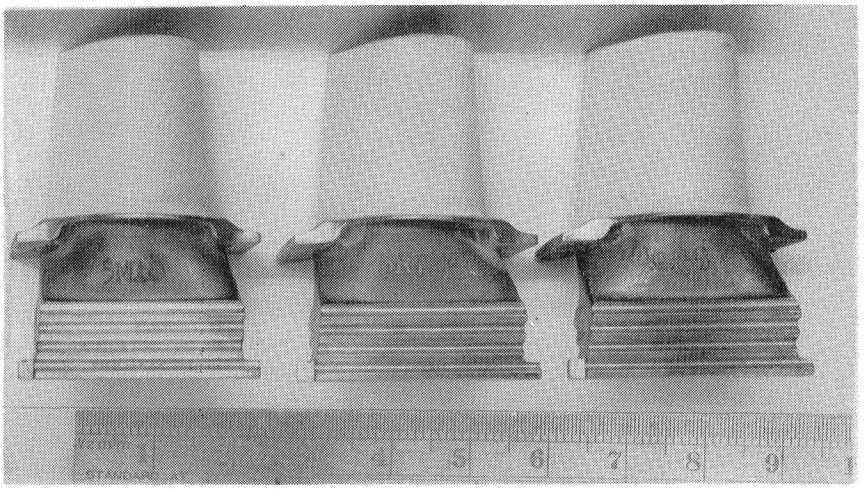

Neg. No. 48591 1X

4 5 6

Figure 7

Appearance of Turbine Blades 1-6 As Received

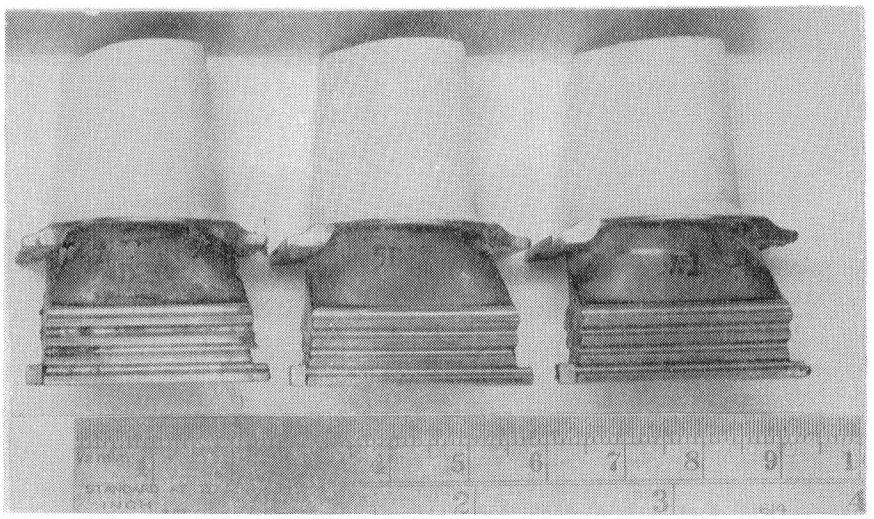

Neg. No. 48590 1X

7 8 9

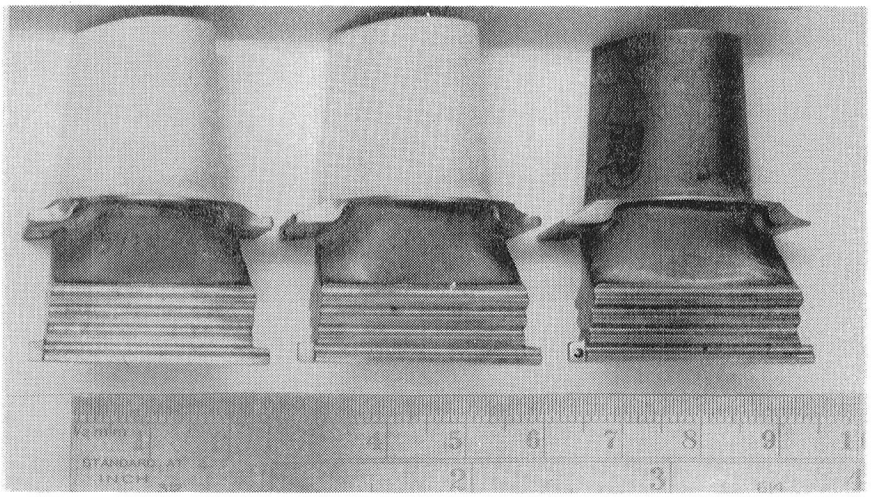

Neg. No. 48589 1X

10 11 12

Figure 8

Appearance of Turbine Blades 7-12 As Received

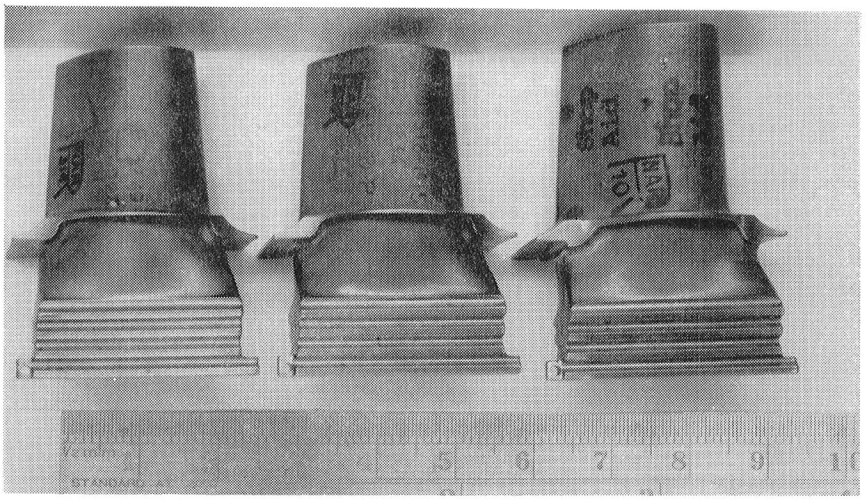

Neg. No. 48588 1X

13 14 15

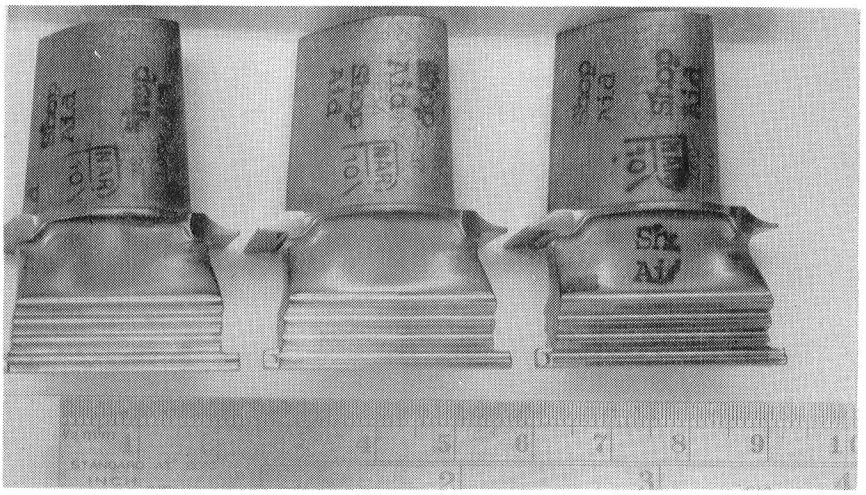

Neg. No. 48587 1X

16 17 18

Figure 9

Appearance of Turbine Blades 13-18 As Received

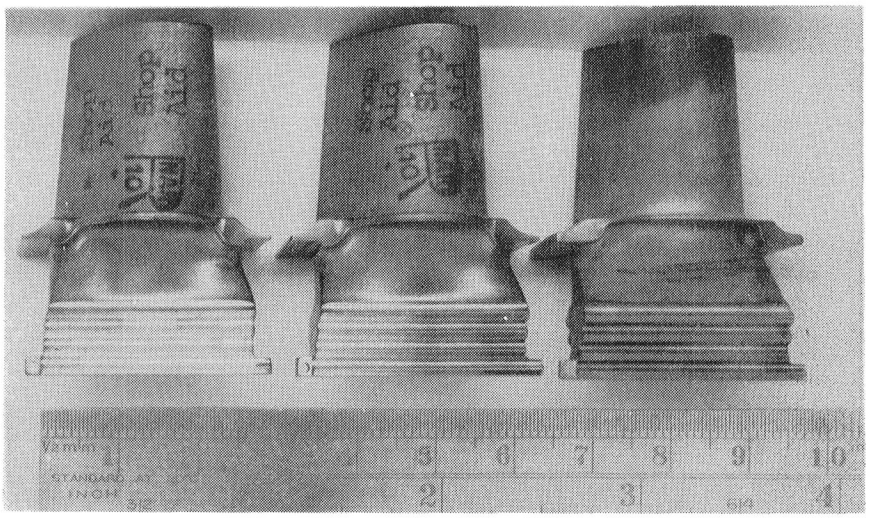

Neg. No. 48586 1X

19 20 21

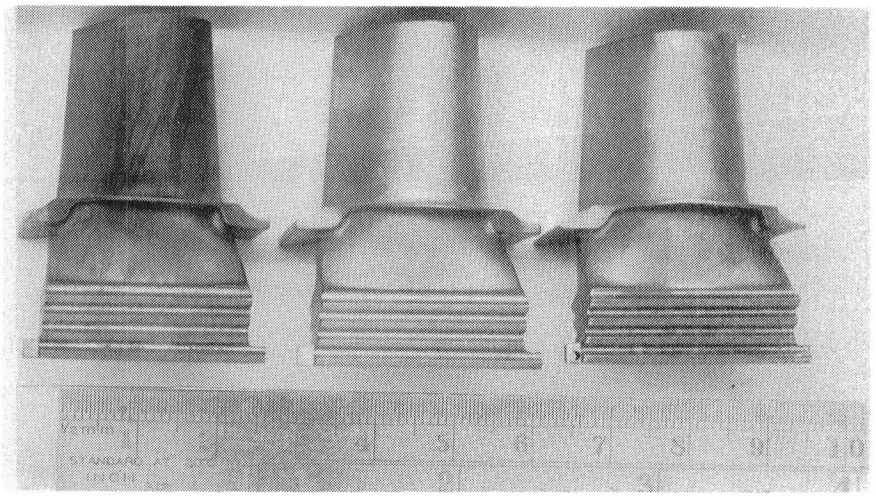

Neg. No. 48485 1X

22 23 24

Figure 10

Appearance of Turbine Blades 19-24 As Received

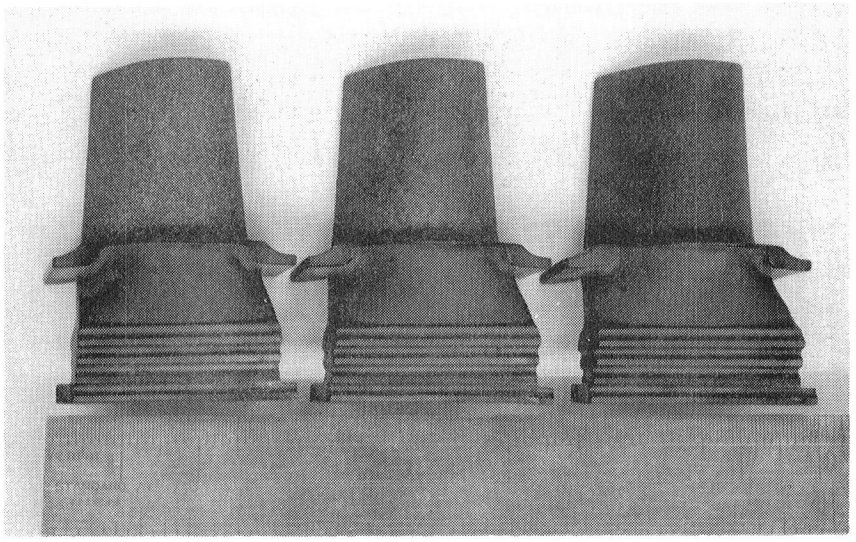

Neg. No. 48931 1X

1 2 3

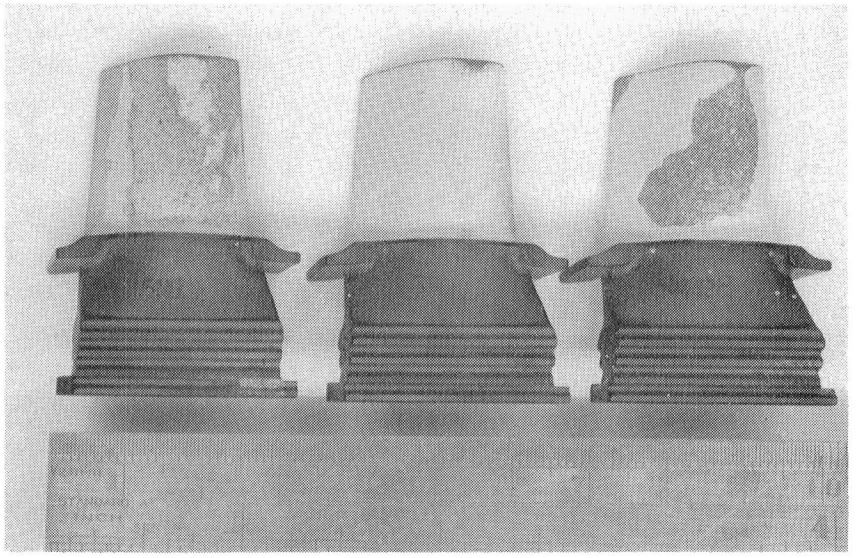

Neg. No. 48930 1X

4 5 6

Figure 11

Appearance of Turbine Blades 1-6 after 3000 Thermal Cycles at 950°/25°C (1742°/77°F). Note spalling of thermal barrier coating on specimens 4 and 6.

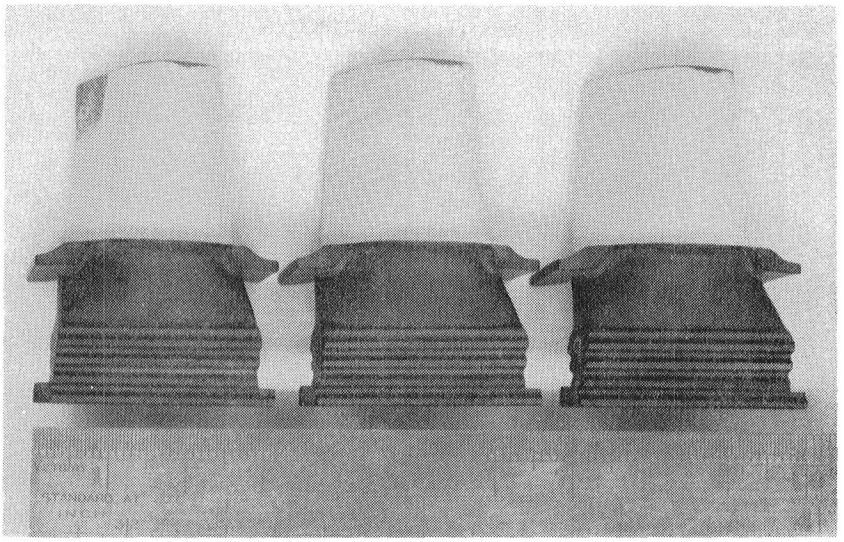

Neg. No. 48929 1X

7 8 9

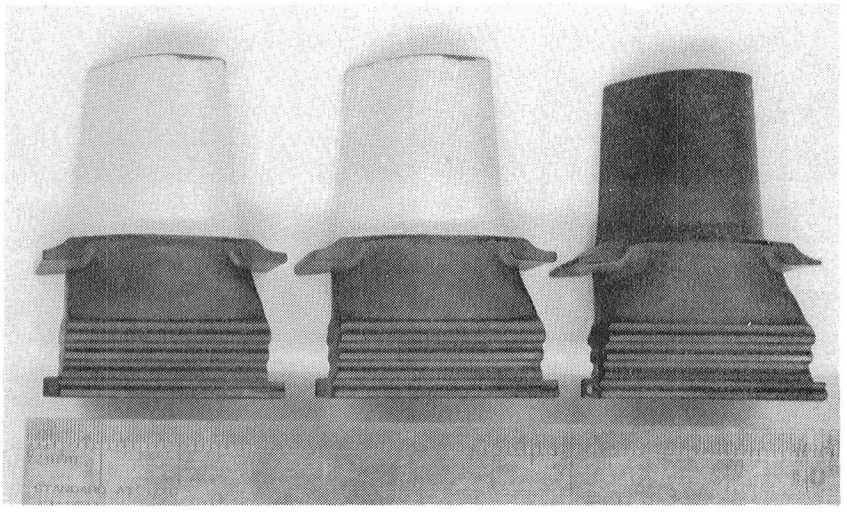

Neg. No. 48928 1X

10 11 12

Figure 12

Appearance of Turbine Blades 7-11 after 3000 Thermal Cycles at 950°/25°C (1742°/77°F)

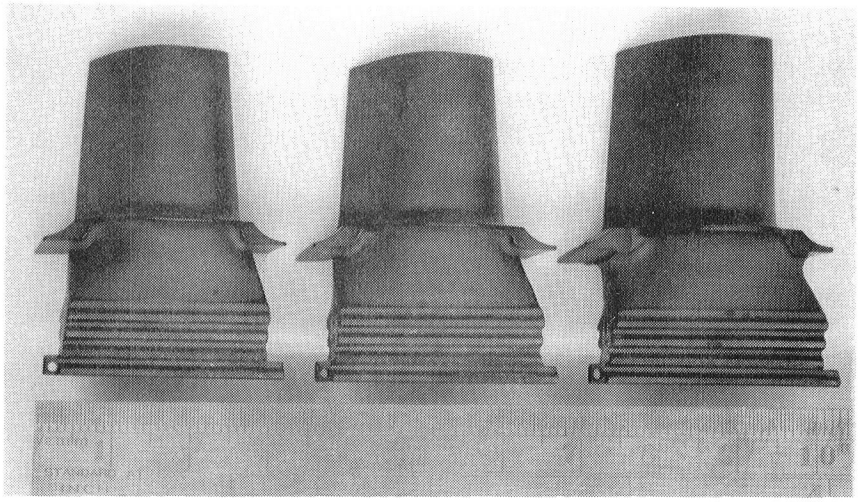

Neg. No. 48927 1X

13 14 15

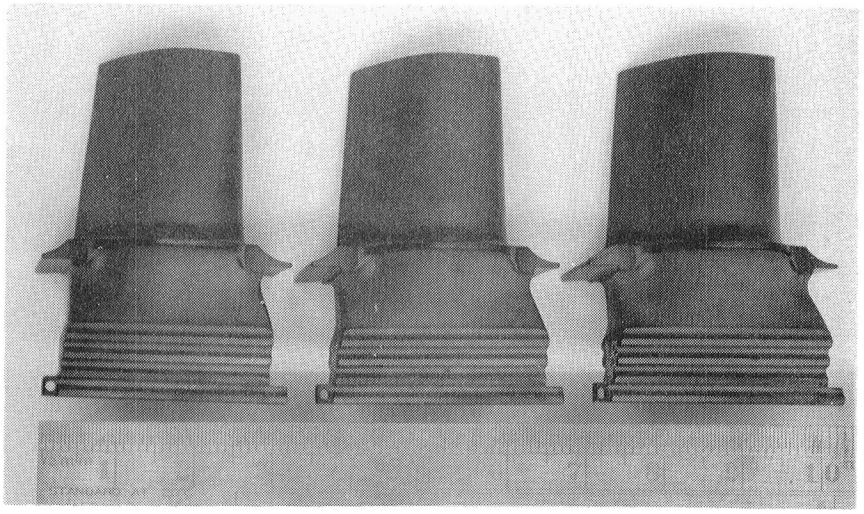

Neg. No. 48926 1X

16 17 18

Figure 13

Appearance of Turbine Blades 13-18 after 3000 Thermal Cycles at 950°/25°C (1742°/77°F)

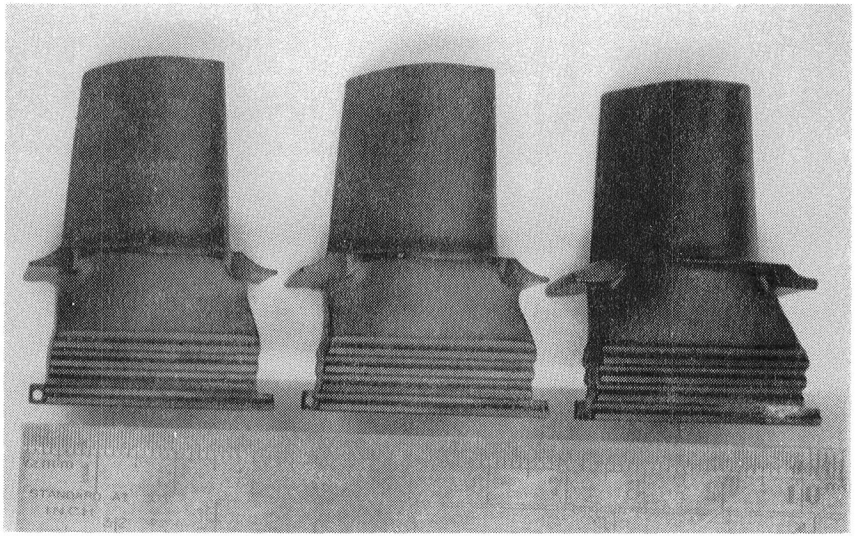

Neg. No. 48925 1X

19 20 21

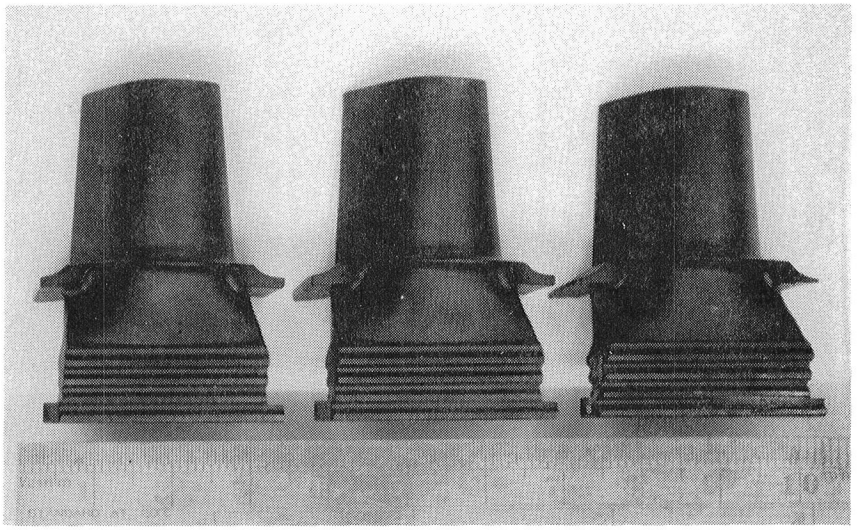

Neg. No. 48924 1X

22 23 24

Figure 14

Appearance of Turbine Blades 19-24 after 3000 Thermal Cycles at 950°/25°C (1742°/77°F)

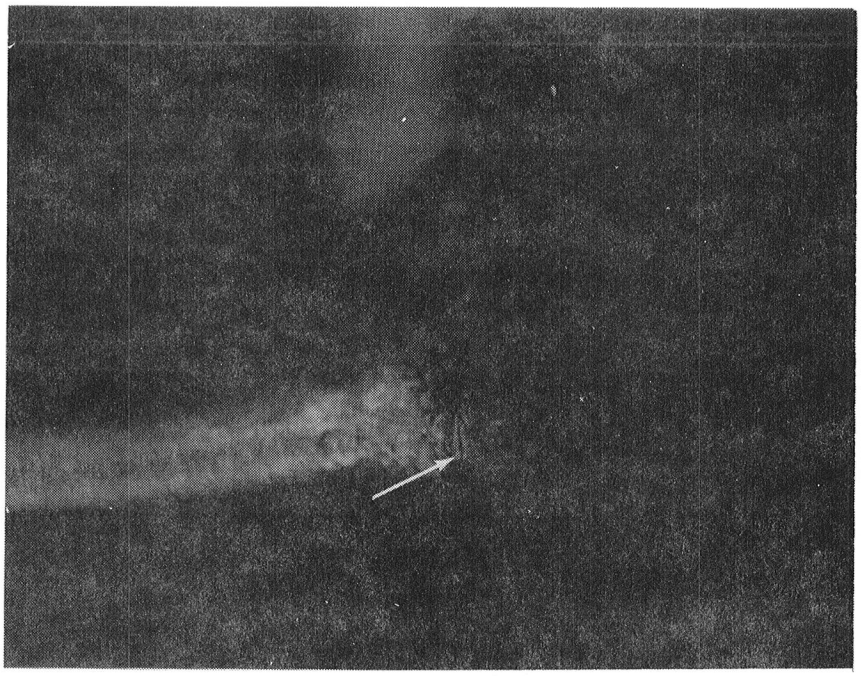

Neg. No. 48966 25X

Blade 15

Neg. No. 48967 25X

Blade 17

Figure 15

Typical Thermal Fatigue Cracks on Trailing Edge Radius at Platform of Turbine Blades 15 and 17

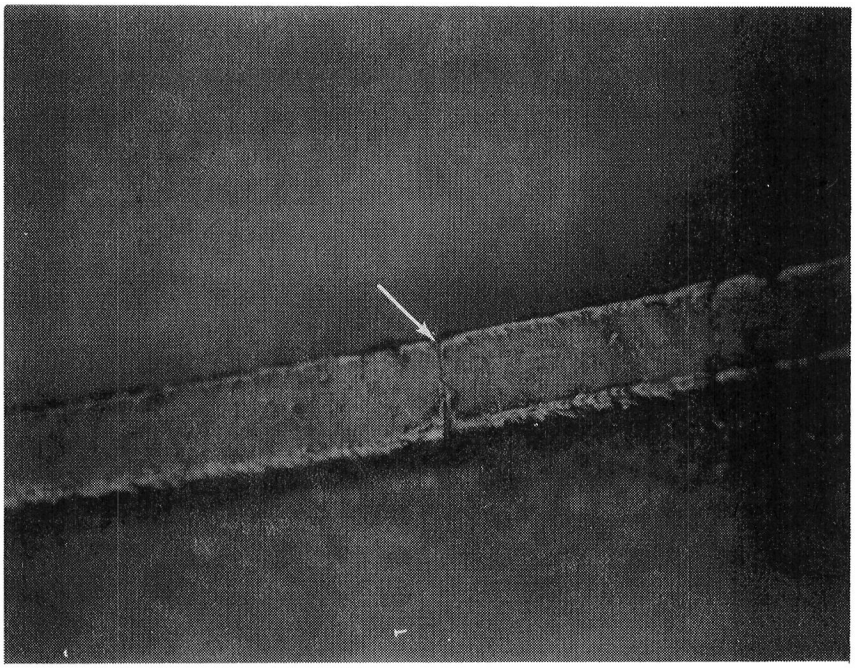

Neg. No. 48973 25X

Blade 12

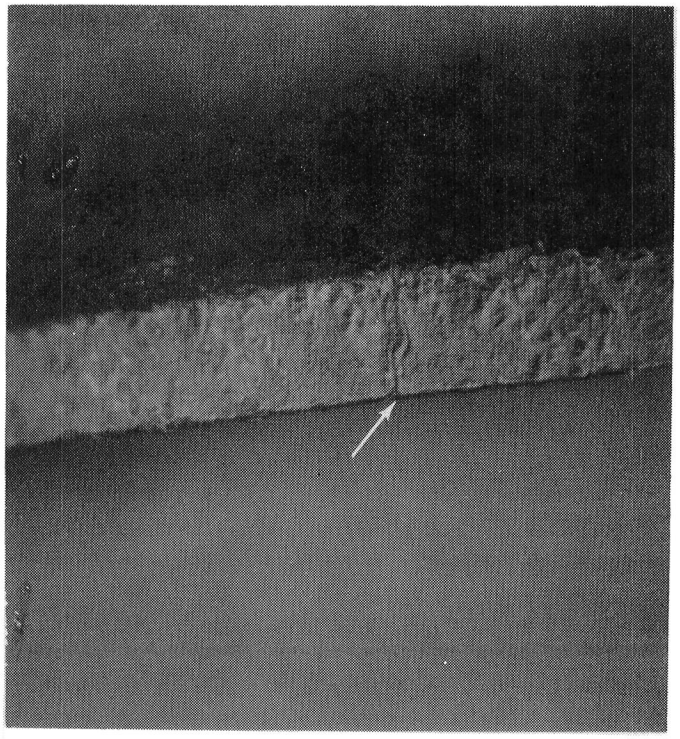

Neg. No. 48932 25X

Blade 21

Figure 16

Typical Thermal Fatigue Cracks on Blade Platform Concave Side of Blades 12 and 21